Surface & Coatings Technology 206 (2012) 3728–3732

Contents lists available at SciVerse ScienceDirect

Surface & Coatings Technology

journal homepage: www.elsevier.com/locate/surfcoat

Galvanic corrosion of Ni–Cu–Al composite coating and its anti-fouling property for metal pipeline in simulated geothermal water

G.G. Wang, L.Q. Zhu, H.C. Liu, W.P. Li *

Key Laboratory of Aerospace Materials and Performance (Ministry of Education), School of Materials Science and Engineering, Beihang University, Beijing 100191, China

ARTICLE INFO

Article history:
Received 17 September 2011
Accepted in revised form 28 February 2012
Available online 6 March 2012

Keywords:
Composite coating
Galvanic corrosion
$CaCO_3$ fouling
Surfaces
Anti-fouling

ABSTRACT

A novel anti-fouling epoxy-silicone composite coating containing Ni–Cu–Al alloy powder for metal pipeline in geothermal water was fabricated based on the basic principles of galvanic corrosion. Fouling behaviors of the surface of composite coating in the simulated geothermal water were studied in comparison with stainless steel and epoxy-silicone resin coating. The results indicated that composite coating possessed a good anti-fouling performance. In the geothermal water, Ni^{2+}, Cu^{2+} and Al^{3+} ions, originated from interface electrochemical corrosion, were released into bulk solution. These metal ions intensively inhibited nucleation and crystal growth rate of $CaCO_3$ fouling on the surface of composite coating, and promoted precipitation of $CaCO_3$ fouling in the bulk-solution, which could be easily washed away by flowing water. But for 304 stainless-steel and epoxy-silicone resin coating, $CaCO_3$ fouling grew easily and adhered firmly to their surfaces, and influenced the transport efficiency of geothermal water for pipelines.

1. Introduction

Since geothermal water contains a lot of corrosion and fouling ions, including Cl^-, Mg^{2+}, Ca^{2+}, HCO_3^- and SO_4^{2-}, metal pipelines and equipments are suffering from serious corrosion and fouling problems in the process of transporting geothermal water, which reduces the efficiency and service life of pipelines, and increases the cost of geothermal energy exploitation[1–4].

Coating technology can effectively protect metal pipelines from corrosion in geothermal water. But the problems of fouling have not been well resolved yet. Until now, many methods have been developed to reduce fouling deposition on pipelines, including coating with low surface energy coatings (PPS/PTFE, Ni-P-PTFE [5–7]), adding chemical reagents in geothermal water [8,9] and electric or magnetic field treatment [10,11]. However, all these methods are subject to certain limitations, such as high cost and secondary pollution [12].

Multiple alloys like KDF, MRPS and Cu–Zn alloy have aroused more interests in anti-fouling researches. After treating geothermal water with the alloys, pipelines showed a good anti-fouling performance to some degree due to the alloy that released Zn^{2+} ions into bulk solution [13]. The Zn^{2+} ions can effectively restrain the crystal growth rate of $CaCO_3$ fouling and change $CaCO_3$ morphology on the pipeline surface [14,15]. Glasner [16] showed that Zn^{2+} and CO_3^{2-} ions in geothermal water spontaneously formed a complex carbonate ion $[Zn(CO_3)_2]^{2-}$, which would be used as nucleation center for the crystallization of $CaCO_3$. Although Zn^{2+} ions would increase the amount of $CaCO_3$ fouling nucleus in bulk solution, the amount of $CaCO_3$ could also be increased on the surface of pipelines. Meanwhile, the preparation of multiple alloys was characteristic of high energy consumption. Hence, multiple alloys used as anti-fouling tools for pipelines exhibit a few limitations.

Coating technology is a simple and cheap method which has been widely used in our daily life. Blending with zinc powder, TiO_2 and dyestuff in slurry coating can obtain functional coatings with anti-corrosion, anti-biosis and decorative performance, respectively [17,18]. Some literatures have indicated that Mg^{2+}, Cu^{2+}, Fe^{2+}, etc. ions can also partially influence the precipitation behavior reduce nucleation and crystal growth rate of $CaCO_3$ fouling in geothermal water [19]. Thus, based on galvanic corrosion of alloy powder in geothermal water, alloy powder blended in slurry coating has potential to be used as a functional coating with good anti-fouling property for pipelines.

In our work, based on the basic principles of galvanic corrosion, nickel–copper–aluminum alloy powder blending epoxy-silicone resin composite coating was designed and its anti-fouling performance in the simulated geothermal water was studied. Compared with stainless steel and epoxy-silicone resin coating, the composite coating showed a good anti-fouling performance. This study might provide a simple, cheap technique to improve the anti-fouling performance of metal pipelines.

2. Experimental procedures

The metallic specimens used were 304 stainless-steel which was 38 mm in out-diameter, 2.5 mm in wall thickness. All the chemical

* Corresponding author. Tel.: +86 1082317113; fax: +86 1082317133.
E-mail address: liweiping@mse.buaa.edu.cn (W.P. Li).

0257-8972/$ – see front matter © 2012 Elsevier B.V. All rights reserved.
doi:10.1016/j.surfcoat.2012.02.054

reagents and solvents were of analytical grade. W304 epoxy-silicone resin for the slurry coating was supplied by Yuanen Composition material Co., Ltd. Flake aluminum powders blended in W304 epoxy-silicone resin slurry have a flat shape of not more than 16 μm in thickness. The copper and nickel powders were 6–8 μm and 2–4 μm in diameter, respectively. The simulated geothermal water at 50 °C was used as the medium to characterize the anti-fouling property. The chemistry compositions of the simulated geothermal water were as shows in Table 1.

Flake aluminum blended cooper and nickel powder with a constant cooper/nickel/aluminum ratio of 1/1/0.1 by weight was prepared in a rotary blender. The base resin solution was prepared by mixing 66.7 vol.% epoxy-silicone resin with 33.3 vol.% dimethylbenzene. And 35 wt.% blended powders were mixed with 65 wt.% the base resin solution to make the alloy powder blending epoxy-silicone resin composite slurry coating. The stainless steel specimens were treated in the processes of oil removal and grounded by 180# SiC abrasive paper, flushed by deionized water, dried by cool air and brushed with the slurry coatings. The slurry-wetted stainless steel specimens were preheated in an air oven at 70 °C for 20 min, then heated at 180 °C for 60 min followed by cooling to room temperature in air environment.

The coated and non-coated stainless steel specimens were vertically immersed in different vessels containing 500 ml simulated geothermal water without stirring at 50 °C. The morphology and the elemental distribution of the specimens and fouling were characterized by SEM (JSM-530) equipped with EDS. The phase structure was examined by XRD (Rigaku 2000). The concentration of calcium ions in simulated geothermal water was quantitatively assayed by EDTA titrimetric analysis according to the Chinese standard (GB 7476-87).

3. Result and discussion

Since the simulated geothermal water contains supersaturated Ca^{2+} and HCO_3^- ions, there are three-step reactions will occur as follows:

$$HCO_{3\,(aq)}^- \leftrightarrow OH^-_{(aq)} + CO_{2(aq)}$$
$$OH^-_{(aq)} + HCO_{3\,(aq)}^- \leftrightarrow CO_{3\,(aq)}^{2-} + H_2O$$
$$Ca^{2+}_{(aq)} + CO_{3\,(aq)}^{2-} \leftrightarrow CaCO_{3(s)}$$

Once the second reaction occurred, CO_3^{2-} ions react spontaneously with Ca^{2+} ions to form nucleation of $CaCO_3$ fouling in bulk solution and on the surface of pipeline [21]. It is known that fouling adhered to the surface of pipelines would influence their transport efficiency. However, fouling precipitating in bulk solution is harmless to pipelines because they could be washed away by flow water.

It is known that nucleation and crystal growth rate are usually divided into induction period and crystal growth period. An amount of fouling adhered to the surface of pipeline and precipitating in bulk solution has a direct relationship to their induction period of crystal nucleation and crystal growth rate: The amount of fouling would increase when the induction period of crystal nucleation decreases or crystal growth rate increases.

In the simulated geothermal water, galvanic corrosion of galvanic couple composed of Ni–Cu, Ni–Al, Cu–Al and Ni–Cu–Al would occur on the surface of composite coating because nickel, copper and aluminum powder have different electrode potential (φ_{Ni}—0.136 *V*, φ_{Cu} + 0.337 *V*, φ_{Al}—1.66 *V*)[22]. Among these galvanic couple, nickel and aluminum powder due to their lower electrode potential would be the top priority to being oxidized to Ni^{2+} and Al^{3+} ions that would diffuse into bulk solution. Although aluminum powder of Cu–Al, Ni–Al and Ni–Cu–Al galvanic couples are easily oxidized, the corrosion process of aluminum powder would be stopped or slowed because of compact oxidation film produced from the galvanic corrosion covering on aluminum powder surface. And the copper and nickel powder would also be corroded in water. Hence, in the simulated geothermal water, galvanic corrosion reactions occurring on the surface of composite coating are as follows:

$$\text{Anode: } Ni \rightarrow Ni^{2+} + 2e;\ Cu \rightarrow Cu^{2+} + 2e;\ Al \rightarrow Al^{3+} + 3e$$
$$\text{Cathode: } O_2 + H_2O + 4\,e \rightarrow 4OH^-$$

These galvanic corrosion reactions cause Ni^{2+}, Cu^{2+} and Al^{3+} ions cumulate in the vicinity of composite coating. Besides, being driven by the ion concentration gradient, there would be an amount of Ni^{2+}, Cu^{2+} and Al^{3+} ions in bulk solution. Those metal ions intensively inhibit the nucleation and crystal growth rate of $CaCO_3$ fouling precipitating on the surface of composite coating and anti-fouling performance of composite coating would be improved. Furthermore, with galvanic corrosion reactions progress, some of those metal ions would react with O_2, CO_3^{2-} etc. in the simulated geothermal water to form corrosion products and cover on the surface of composite coating. Due to the existence of the corrosion products, further corrosion of composite coating would be stopped or slowed.

Fig. 1 illustrates the surface of specimens after being immersed in the simulated geothermal water for 72 h. It can be seen that the surface of stainless steel and epoxy-silicone resin coating are covered with a large amount of needle-like matters. And the single needle adhered to stainless steel and epoxy-silicone resin coating is 40–60 μm and 70–100 μm in length, respectively. The analysis of EDS (Table 2(1) and Table 2(2)) and our previous work reveal that needle-like matters are the classical aragonite fouling in geothermal water [23,24]. However, compared with the surface of composite coating before immersion (Fig. 1c), stainless steel and epoxy-silicone resin coating, there are no obvious changes except a little of needle-like matter with 8–12 μm in length covering on composite coating surface after immersion (Fig. 1d). The analysis of EDS (Table 2(3)) shows that the needle-like matter is $CaCO_3$. These results indicate that Ni^{2+}, Cu^{2+} and Al^{3+} ions produced from interface galvanic corrosion intensively inhibit induction period of crystal nucleation and crystal growth rate of $CaCO_3$ fouling precipitating on the surface of composite coating. According to magnified image of Fig. 1d, flake aluminum powder of composite coating becomes rough after immersion due to the covering of a larger amount of small ball-like matters. The analysis of EDS (Table 2(4)) shows that ball-like matters are composed of C, O, Al, Ni, Cu elements accompanied by a small amount of Mg element, and Ca element is not detected. These are due to corrosion products produced from galvanic corrosion covering on the surface of composite coating. The existence of corrosion products would slow the galvanic corrosion of alloy powder in the simulated geothermal water.

The XRD patterns for the surface of composite coating before and after immersion in the simulated geothermal water are shown in Fig. 2. According to Fig. 2, the diffraction peaks indicate that phases of composite coating surface mainly are nickel, copper and aluminum pure phases after immersion. No obvious characteristic peaks of $CaCO_3$ are found, also suggesting that almost no fouling covers on the surface of composite coating. Besides, due to a little amount of metallic oxide and other compounds covering on the surface of composite coating, their characteristic peaks could not be obviously seen in the XRD patterns.

Increasing the immersion time of specimens in the simulated geothermal water to 168 h, needle-like $CaCO_3$ fouling covering on the

Table 1
Compositions of simulated geothermal water [20].

Composition	Na^+	SO_4^{2-}	Mg^{2+}	Ca^{2+}	K^+	HCO_3^-	Cl^-	pH
Contain (g/L)	1.559	0.076	0.039	0.102	0.093	0.241	2.59	6–7

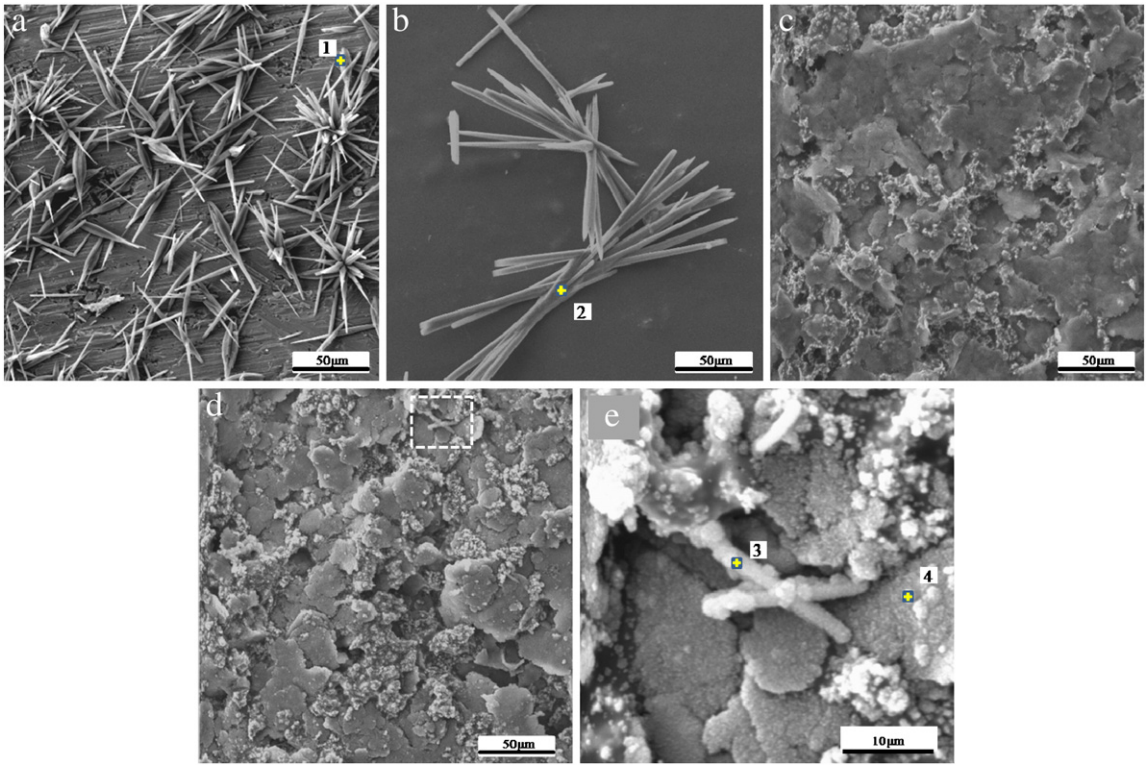

Fig. 1. SEM images for the surface of specimens after immersion in the simulated geothermal water: a) stainless steel; b) epoxy-silicone resin coating; d) composite coating; c) composite coating before immersion; e) magnified image of Fig. 1d.

surface of stainless steel becomes bigger and longer (Fig. 3b). Besides, a little of needle-like $CaCO_3$ fouling can be seen on the surface of composite coating (Fig. 3a). However, an amount of $CaCO_3$ fouling adhering to the surface of composite coating is still much smaller than that adhering to stainless steel surface, meaning that composite coating reveals a good anti-fouling performance. In conclusion, due to the existence of those metal ions, nucleation, crystal growth rate of $CaCO_3$ fouling and an amount of nucleation numbers adhering to the surface of composite coating become lower and smaller, respectively.

Fig. 4 shows the SEM images of stainless steels being immersed in different test vessel for 72 h. According to our previous work [25], an amount of fouling adhered to the surface of stainless steel can reflect an amount of fouling precipitating in bulk solution in some degree. According to Fig. 4a, $CaCO_3$ fouling on stainless steel is too sparse to cover the whole surface. However, due to the existence of composite coating, the surface of stainless steel is almost entirely covered because of the dense growth of needle-like $CaCO_3$ fouling (Fig. 4b). This means that nucleation and crystal growth process of $CaCO_3$ fouling are easy in bulk solution.

That $CaCO_3$ fouling easily precipitate in bulk solution may be probably due to the Ni^{2+}, Cu^{2+}, Al^{3+} ions produced from galvanic corrosion in bulk solution. As mentioned above, Zn^{2+} and CO_3^{2-} ions in geothermal water spontaneously form a complex carbonate ion $[Zn(CO_3)_2]^{2-}$, which would be used as the nucleation center for crystallization of $CaCO_3$[16]. According to our previous work[25], the Ni^{2+}, Cu^{2+}, Al^{3+} ions in bulk solution might be probably similar to Zn^{2+} ion and combine with CO_3^{2-} to form a complex carbonate, which can work as the nucleation accelerators of $CaCO_3$ and boost the formation of $CaCO_3$ fouling in the bulk solution. High concentration of Ni^{2+}, Cu^{2+} and Al^{3+} ions cumulated in the vicinity of composite coating would form a strong barrier to Ca^{2+} as the electrostatic repulsion. Besides, high concentration of those metal ions would intensively inhibit nucleation and crystal growth rate of

Table 2
EDS analysis of products on the surface of different specimens.

Element/weight percent (wt.%)	C	O	Ca	Fe	Al	Ni	Cu	Mg
(1)	16.52	33.86	49.62	–	–	–	–	–
(2)	11.23	23.67	61.99	3.11	–	–	–	–
(3)	10.2	19	15.23	–	28.04	12.27	15.26	–
(4)	9.63	18.80	–	–	39.76	18.97	11.11	1.73

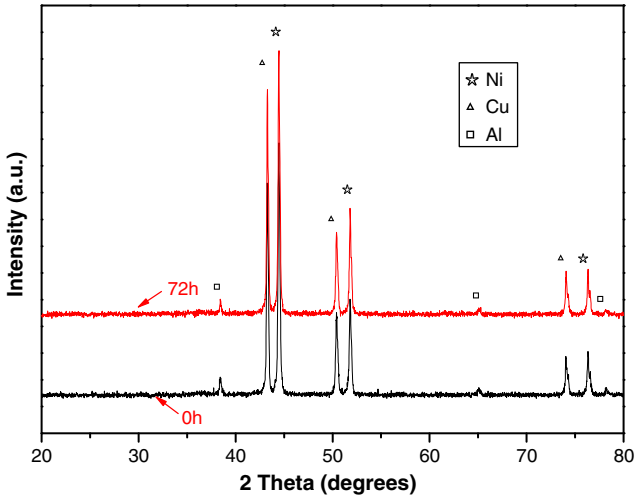

Fig. 2. XRD patterns for the surface of composite coating before and after immersion in the simulated geothermal water for 72 h.

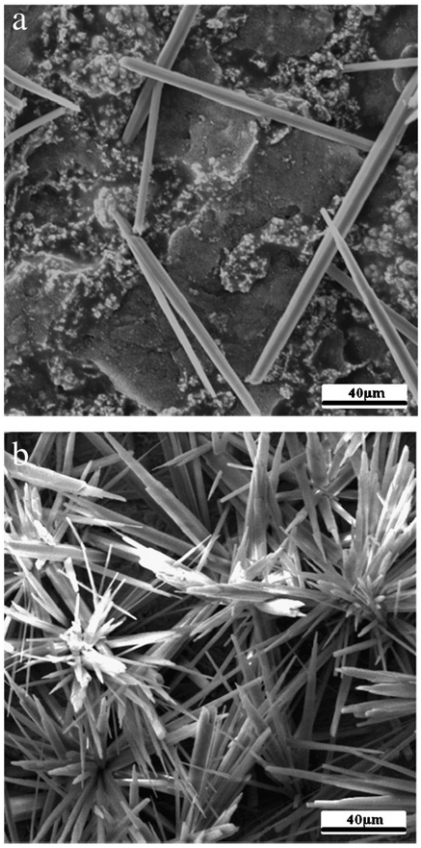

Fig. 3. SEM images for the surface of specimens after immersion in the simulated geothermal water for 168 h: a) composite coating; b) stainless steel.

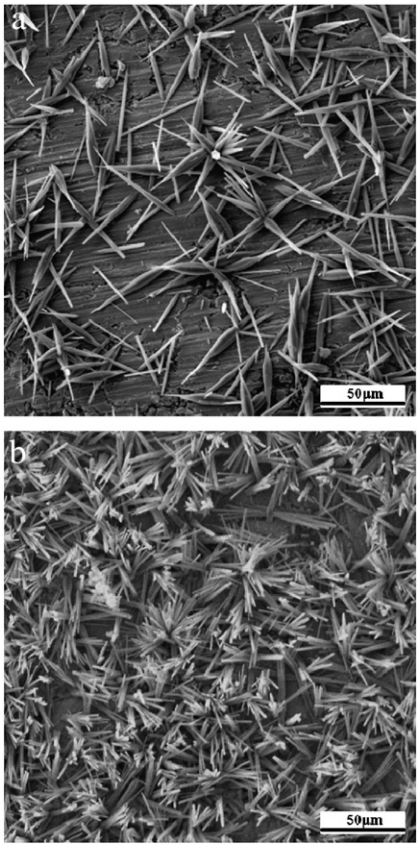

Fig. 4. SEM images of specimens immersed in different test vessel for 72 h. (a) Stainless steel; (b) stainless steel with the composite coating after immersion in the same test vessel.

$CaCO_3$ fouling on the surface of composite coating [19,26,27]. Therefore, due to the existence of composite coating, $CaCO_3$ fouling easily precipitates in the bulk solution instead of on the surface of composite coating. Compared with stainless steel and epoxy-silicone resin coating, composite coating shows a good anti-fouling performance in geothermal water.

Fig. 5 shows the variations of Ca^{2+} concentration with time in the simulated geothermal water. The decrease in the concentration of Ca^{2+} ions in solution containing composite coating is greater than that in the solution containing stainless steel. After immersion in the simulated geothermal water for 72 h, the concentration of Ca^{2+} ions in the solutions containing composite coating and stainless steel decrease to 30.1 mg/L and 45.3 mg/L, respectively. It can be calculated that about 71.5 mg $CaCO_3$ fouling precipitated in the solution containing composite coating and about 52.5 mg $CaCO_3$ fouling precipitated in the solution containing stainless steel. However, it has been discussed that only little $CaCO_3$ fouling adhering to the surface of composite coating as shown in Fig. 1d. Therefore, these can also prove that $CaCO_3$ fouling is prone to precipitate in bulk solution rather than on the surface of composite coating due to the existence of composite coating in the simulated geothermal water.

4. Conclusion

Based on the principles of galvanic corrosion, a novel anti-fouling composite coating containing Ni–Cu–Al alloy powder for metal pipelines in the simulated geothermal water has been studied. When composite coating was immersed in the simulated geothermal water, galvanic corrosion of galvanic couples including Ni–Cu, Ni–Al, Cu–Al and Ni–Cu–Al would occur and release Ni^{2+}, Cu^{2+} and Al^{3+} ions into bulk solution. With the influences of metal ions on the induction period of crystal nucleation and the crystal growth rate of $CaCO_3$ fouling, $CaCO_3$ fouling was prone to precipitate in bulk solution rather than on the surface of composite coating. Besides, the corrosion products produced from electrochemical corrosion would cover on the surface of composite coating and slow the further corrosion of composite coating.

After being immersed in the simulated geothermal water at 50 °C for 72 h, compared with stainless steel and epoxy-silicone resin coating, only a small amount of fouling was observed on the surface of composite coating and the composite coating showed a good anti-fouling performance. This study might provide a simple, cheap technique to improve the anti-fouling performance of metal pipelines.

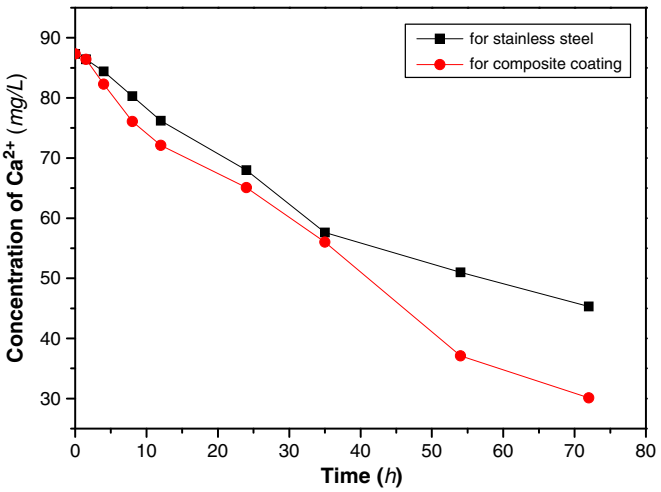

Fig. 5. Concentration of Ca^{2+} ions were determined according to Chinese Standard GB 7476–87.

References

[1] K.H. Wu, L.Q. Zhu, W.P. Li, H.C. Liu, Corros. Sci. 52 (2010) 2244.
[2] L.Q. Zhu, K.H. Wu, W.P. Li, H.C. Liu, Acta Phys. Chim. Sin. 26 (2010) 39.
[3] D.L. Gallupa, F. Sugiamanb, V. Capunoc, Appl. Geochem. 18 (2003) 1597.
[4] Y.H. Cheng, Y. Zou, L. Cheng, W. Liu, Surf. Coat.Technol. 203 (2009) 1559.
[5] T. Sugama, K. Gawlik, Mater. Lett. 57 (2002) 666.
[6] K.H. Wu, W.P. Li, H.C. Liu, L.Q. Zhu, J. Univ. Sci. Tech. Beijing 31 (2009) 1263.
[7] Q. Zhao, Y. Liu, H. Muller-Steinhagen, G. Liu, Surf. Coat.Technol. 155 (2002) 279.
[8] X.G. Wang, W.W. Qi, X.W. Zhang, T. Sun, J. Northeast. Univ. (Nat. Sci.) 31 (2010) 909.
[9] R. Ketrane, B. Saidani, O. Gil, L. Leleyter, F. Baraud, Desalination 249 (2009) 1397.
[10] Y.T. Clifford, M.C. Chang, R.J. Shieh, T.G. Chen, J. Cryst. Growth 310 (2008) 3690.
[11] L.D. Tijing, H.Y. Kim, D.H. Lee, C.S. Kim, Y.I. Cho, Int. J. Heat Mass Transf. 53 (2010) 1426.
[12] Q.F. Yang, j. Ding, Z.Q. Shen, Chem. Eng. Sci. 55 (2000) 797.
[13] Y.G. He, W.Y. Wang, N. Zhong, G.Y. Zhang, Mate. Sci. Technol. 17 (2009) 810.
[14] Q.G. Tanga, J.P. Meng, J.S. Lianga, L. Niea, Y.X. Li, J. Alloy. Comp. 49 (2010) 242.
[15] S. Ghizellaoui, M. Euvrard, Desalination 220 (2008) 394.
[16] A. Glasner, D. Weiss, J. Inorg. Nucl. Chem. 5 (1980) 655.
[17] L. Straka, H. Kawakami, J. Romu, R. Ilola, R. Mahlberg, Thin Solid Films 517 (2009) 3797.
[18] H.L. Hua, N. Li, J.N. Cheng, L.J. Chen, J. Alloy. Comp. 472 (2009) 219.
[19] E. López-Sandoval, C. Vázquez-López, Desalination 217 (2007) 85.
[20] L.Q. Zhu, K.H. Wu, W.P. Li, H.C. Liu, J. Funct. Mate 41 (2010) 1046.
[21] G.J. Lee, L.D. Tijing, C.B. Pak, B.J. Baek, Y.I. Cho, Int. Commun. Heat Mass Transf. 33 (2006) 14.
[22] G.L. Song, B. Johannesson, S. Hapugoda, D. StJohn, Corros. Sci. 46 (2004) 955.
[23] D.J. Choi, S.J. You, J.G. Kim, Mater. Sci. Eng. A 335 (2002) 228.
[24] L.C. Lipus, D. Dobersek, Chem. Eng. Sci. 62 (2007) 2089.
[25] G.G. Wang, L.Q. Zhu, H.C. Liu, W.P. Li, Mater. Let. 65 (2011) 3095.
[26] H. Meyer, J. Cryst Growth 66 (1984) 639.
[27] S. Ghizellaoui, M. Euvrard, J. Ledion, A. Chibani, Desalination 206 (2007) 185.